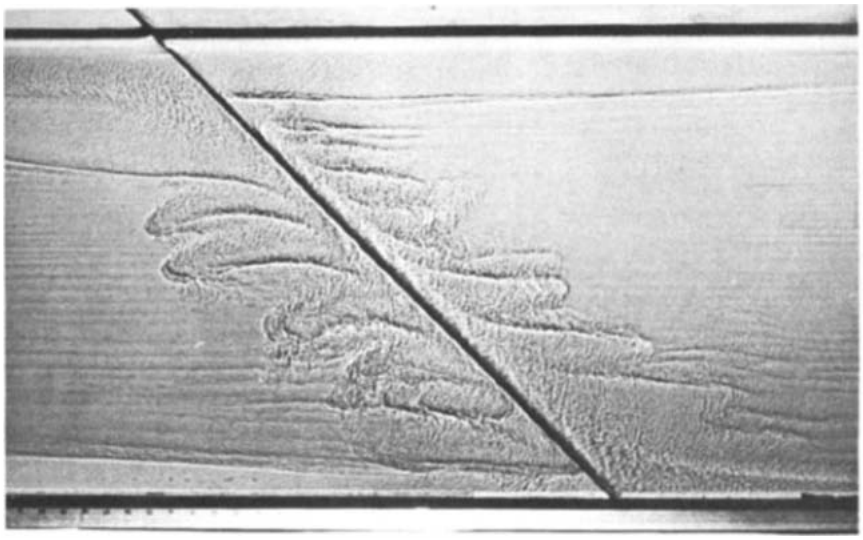

Figure 3.12: Sloping layered convection (Turner 1974).

dynamic stability limit: so nothing should happen. However, if a sloping boundary exists as shown, convection is initiated, and takes the layered form shown. We leave it as an exercise to explain why.

3.7 Turbulence

Many forms of convection involve turbulent flow, namely when the Reynolds number and the Rayleigh number are sufficiently large (i.e. for strong inertia). For example, the hot smoke rising from a flame can often be seen to transition from a smooth laminar regime to a chaotic turbulent regime as it accelerates due to buoyancy. Similarly, plumes arising from heat sources in buildings often transition to turbulence as they rise towards the ceiling, before cooling and recirculating. Hence, in this section we briefly outline some of the fundamentals of turbulent flows as well as common modelling techniques. Much of the following section has been taken from the introduction of (Benham, *DPhil thesis* (2018)). For further reading, see the books by Schlichting (1960), Jimenez (2000) and Pope (2000).

We start by reminding ourselves of the dimensionless Navier-Stokes equations (ignoring buoyancy for the moment), which are

$$\begin{aligned} \nabla \cdot \mathbf{u} &= 0, \\ \frac{\partial \mathbf{u}}{\partial t} + (\mathbf{u} \cdot \nabla)\,\mathbf{u} &= -\nabla p + \frac{1}{\mathrm{Re}} \nabla^2 \mathbf{u}, \end{aligned} \tag{3.79}$$

where $\mathrm{Re} = \rho U_0 L/\mu$ for some typical velocity and length scales U_0, L. We consider high Reynolds number flows $\mathrm{Re} \gg 1$ where inertia is important. In particular, for these flows, the non-linear inertial terms on the left hand side of the Navier-Stokes

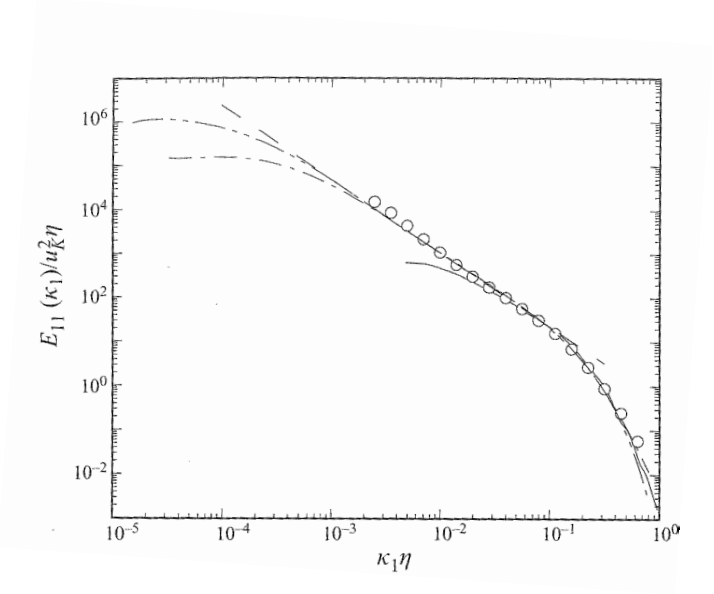

Figure 3.13: Dimensionless energy spectrum (one-dimensional) in terms of dimensionless wavenumber for turbulent flow. This image is taken from (Jimenez (2000)).

equations are responsible for complex flow behaviour, also known as turbulence, which is characteristic of the high Reynolds number regime.

One of the characteristic features of turbulent flows is the mechanism through which energy is transferred between eddies. Although at high Reynolds number viscous terms appear to be negligible (see (3.79)), turbulence is in fact dissipative. It does not, however, dissipate energy at the large scale, like laminar flows. Instead, energy is exchanged in an inviscid way between eddies of diminishing size. Energy is only dissipated (i.e. converted to heat) due to eddies which are so small that viscous effects become important. This critical size is called the Kolmogorov length scale and is given by

$$\eta = \left(\frac{\nu^3}{\varepsilon}\right)^{1/4}, \tag{3.80}$$

where ε is the turbulent energy dissipation and ν is the kinematic viscosity $\nu = \mu/\rho$. When modelling turbulence, it is necessary to account for many different length scales, from the Kolmogorov scale η up to the dominant length scale of the problem L, which can be problematic for computations. The energy spectrum for turbulent flow is shown in figure 3.13, illustrating how energy is transferred from small wavenumbers (large wavelengths) down to large wavenumbers (small wavelengths). This transfer of energy from the large to the small scale, also known as the *energy cascade*, was first described by Kolmogorov (1941). In this famous paper Kolmogorov derived a scaling relationship between the energy of the eddies and their wavenumber $E \propto \kappa^{-5/3}$, showing close agreement with experimental data.

Re	Spatial steps		Time steps	Total	
	2D	3D		2D	3D
10^3	3.2×10^4	5.6×10^6	1.8×10^2	5.6×10^6	1.0×10^9
10^4	1.0×10^6	1.0×10^9	1.0×10^3	1.0×10^9	1.0×10^{12}
10^5	3.2×10^7	1.8×10^{11}	5.6×10^3	1.8×10^{11}	1.0×10^{15}
10^6	1.0×10^9	3.2×10^{13}	3.2×10^4	3.2×10^{13}	1.0×10^{18}

Table 3.1: Minimum number of spatial and time steps for DNS in two and three-dimensional flows at different Reynolds numbers.

In order to solve (3.79) numerically (with suitable boundary conditions), which is known as Direct Numerical Simulation (DNS), the domain is discretised spatially with step size Δx. Let us assume that there are N elements along each dimension of the domain, such that

$$N\Delta x = L. \tag{3.81}$$

Making sure that the smallest eddies are resolved, we must choose $\Delta x \leq \eta$. According to an equilibrium-based scaling law, the energy dissipation obeys the self-similar relationship (i.e. across scales)

$$\varepsilon \approx \frac{{u_L}^3}{L} \approx \frac{\tilde{u}^3}{\eta}, \tag{3.82}$$

where u_L, $\tilde{u}$ are the velocity scales associated with the largest and smallest (Kolmogorov) eddies. Therefore, if we redefine the Reynolds number in terms of u_L, the Kolmogorov length scale is written in dimensionless form as $\eta/L = \mathrm{Re}^{-3/4}$. Hence, the number of spatial steps must be

$$N \geq \mathrm{Re}^{3/4}. \tag{3.83}$$

Therefore, the number of steps for a two dimensional domain scales like $N^2 \sim \mathrm{Re}^{3/2}$, and like $N^3 \sim \mathrm{Re}^{9/4}$ for a three-dimensional domain. To make things worse, we must also consider the number of discretisation points in time. Since memory storage requirements (due to spatial discretisation) are very large at high Reynolds numbers, integration of the solution in time is usually performed using an explicit method. For explicit methods with time step Δt, the Courant-Friedrichs-Lewy (CFL) condition

$$\frac{u_L \Delta t}{\Delta x} < 1, \tag{3.84}$$

must hold in order to achieve stability. If we take $\tau = L/u_L$ as the timescale of interest for the flow, then the number of time steps N_t is given by

$$N_t \Delta t = \frac{L}{u_L}. \tag{3.85}$$

Hence, the CFL condition (3.84) implies

$$N_t \geq \mathrm{Re}^{3/4}. \tag{3.86}$$

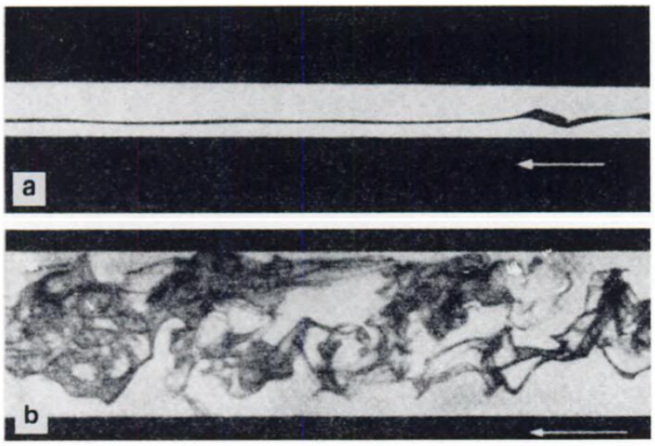

Figure 3.14: Illustration of the difference between laminar flow (a) at Reynolds number Re = 1150 and turbulent flow (b) at Reynolds number Re = 2520. This image is taken from Dubs (1939), which describes the coloured filament experiments of Reynolds (1883).

In Table 3.1 we display the minimum number of spatial and time steps necessary to perform DNS at Reynolds numbers between $\mathrm{Re} = 10^3$ and $\mathrm{Re} = 10^6$. It is clear that DNS becomes incredibly computationally intensive at even moderately high Reynolds numbers for both two and three-dimensional problems, though three-dimensional problems are much worse. For example, if we cap the number of degrees of freedom at 10^{10}, which is still a very computationally demanding procedure, then $\mathrm{Re} > 2.8 \times 10^4$ becomes intractable for two-dimensional flows and $\mathrm{Re} > 2.2 \times 10^3$ for three-dimensional flows.

Reynolds exhibited the disruptive and chaotic qualities of turbulence in 1883 with a coloured dye experiment (see Figure 3.14). He concluded that it would be almost impossible to model flow characteristics exactly and introduced the idea of averaging the Navier-Stokes equations over time. Such approaches are known as Reynolds-averaged Navier-Stokes (RANS) modelling. Let us define the time-averaging of a function f as

$$\bar{f} = \lim_{T \to \infty} \frac{1}{T} \int_0^T f(t)\, dt. \tag{3.87}$$

We split all variables into a time-dependant part, which corresponds to turbulent fluctuations, and a time-averaged part, such that

$$\begin{aligned} u_i &= U_i(x, y, z) + u_i'(x, y, z, t), \quad i = 1, 2, 3, \\ p &= P(x, y, z) + p'(x, y, z, t), \end{aligned} \tag{3.88}$$

where subscripts $1, 2, 3$ correspond to coordinate directions x, y, z. We define the

fluctuating parts to have zero mean, such that

$$\begin{aligned} \overline{u_i'} &= 0, \quad i = 1, 2, 3, \\ \overline{p_i'} &= 0. \end{aligned} \tag{3.89}$$

This decomposition into mean and fluctuating parts is known as the Reynolds decomposition.

By inserting (3.88) into the continuity equation and averaging, we see that this equation is preserved for both the mean and fluctuating parts of the velocity

$$\begin{aligned} \frac{\partial U_i}{\partial x_i} &= 0, \\ \frac{\partial u_i'}{\partial x_i} &= 0, \end{aligned} \tag{3.90}$$

where we sum over the indices using Einstein notation. Similarly, by inserting (3.88) into the dimensional momentum equation and averaging, we get

$$\rho U_j \frac{\partial U_i}{\partial x_j} = -\frac{\partial P}{\partial x_i} + \mu \frac{\partial^2 U_i}{\partial x_j \partial x_j} - \rho \overline{u_j' \frac{\partial u_i'}{\partial x_j}}, \tag{3.91}$$

where the final term on the right hand side is an inertial term due to the turbulent fluctuations. We keep it on the right hand side, together with the viscous stress term, because it represents a stress contribution due to the turbulent fluctuations. Hence, it is known as the Reynolds stress term. It should be noted that

$$\rho \overline{u_j' \frac{\partial u_i'}{\partial x_j}} = \frac{\partial}{\partial x_j} \left[\rho \overline{u_i' u_j'} \right], \tag{3.92}$$

due to (3.90). The Reynolds stress is typically written in terms of an 'eddy viscosity' μ_t and gradients in the mean velocity, such that

$$-\rho \overline{u_i' u_j'} = \mu_t \left[\frac{\partial U_i}{\partial x_j} + \frac{\partial U_j}{\partial x_i} \right]. \tag{3.93}$$

Considering (3.93), the momentum equation (3.91) can be rewritten as

$$\rho U_j \frac{\partial U_i}{\partial x_j} = -\frac{\partial P}{\partial x_i} + \frac{\partial}{\partial x_j} \left((\mu + \mu_t) \left(\frac{\partial U_i}{\partial x_j} + \frac{\partial U_j}{\partial x_i} \right) \right). \tag{3.94}$$

The eddy viscosity plays an important role in turbulence modelling. Whilst in laminar flows, viscous stresses are responsible for the diffusion of momentum, in turbulent flows, it is the eddies and the turbulent fluctuations which are responsible. Therefore, we represent the Reynolds stress as a diffusive term on the right hand side of (3.94), where the diffusion coefficient is the non-linear eddy viscosity.

Equations (3.90a) and (3.94) together are by no means complete. The non-uniqueness of the Reynolds decomposition results in a so-called 'closure problem',

where we are left with too few equations for too many unknowns. Some approaches involve finding higher *moments* of the governing equations. For example, the turbulent kinetic energy is defined as

$$k = \frac{1}{2}\overline{u_i' u_i'}, \tag{3.95}$$

for which a governing equation can be derived my multiplying the Navier-Stokes equations by u_i' and averaging. However, since new variables are introduced, the system remains unclosed, requiring higher and higher moments (an unending process). Typically, turbulence models make an empirical hypothesis for μ_t (and/or k) to close the system. In the next section we discuss one such turbulence closure assumption.

3.7.1 Prandtl mixing length theory

There are a vast number of different turbulence closure models that have been proposed in the literature. These models are largely classified into three different types. The most basic type, known as algebraic models, do not model the turbulent kinetic energy k, but instead use an eddy viscosity μ_t, which is a function of the mean velocity U_i and its gradients alone. In these models, (3.90a) and (3.94) form a complete system of equations. Next we summarise the assumptions of one of these models, known as Prandtl mixing length theory.

In the early 20$^{\text{th}}$ century Ludwig Prandtl suggested a very simple algebraic model for the eddy viscosity which is based on simple scaling laws (Prandtl (1925)). Prandtl mixing length theory states that the kinematic eddy viscosity $\nu_T = \mu_t/\rho$ is proportional to a velocity scale via a mixing length ℓ, such that

$$\nu_T = \ell\, U_0, \tag{3.96}$$

where in simple shear flows the velocity scale is locally determined by the mean velocity gradient

$$U_0 = \ell \left| \frac{\partial U}{\partial y} \right|. \tag{3.97}$$

Therefore, the eddy viscosity is written as

$$\nu_T = \ell^2 \left| \frac{\partial U}{\partial y} \right|. \tag{3.98}$$

The mixing length ℓ can be interpreted as the approximate distance it takes for a parcel of fluid to move before it becomes blended into its surroundings due to turbulent mixing. The mixing length is considered as a variable and it is modelled differently depending on the problem. For example, in wall bounded flows the mixing length may be taken as the distance to the wall. For flow in a mixing layer, the mixing length may be taken as proportional to the width of the mixing layer.

This model provides a good approximation for simple turbulent flows, such as a boundary layer on a flat plate, or a free mixing layer, though may be less accurate for more complicated turbulent flows. Nevertheless, it is one of the few turbulence models which yields simple and useful analytical results. Later we use Prandtl mixing length theory to derive a model for the growth of a turbulent mixing layer.

3.7.2 Turbulent boundary layer equations

Next we discuss the boundary layer approximation to the RANS equations (3.90a) and (3.94), restricting our attention to two-dimensional flows. We scale the variables according to

$$x \sim L, \quad y \sim L\mathrm{Re}^{-1/2}, \quad U \sim U_0, \quad V \sim U_0\mathrm{Re}^{-1/2}, \quad P \sim \rho U_0^2. \tag{3.99}$$

Therefore, to leading order the two-dimensional turbulent boundary layer equations (reverting the variables back to lower case for convenience) are

$$\begin{aligned} \frac{\partial u}{\partial x} + \frac{\partial v}{\partial y} &= 0, \\ u\frac{\partial u}{\partial x} + v\frac{\partial u}{\partial y} &= -\frac{1}{\rho}\frac{\partial p}{\partial x} + \frac{\partial}{\partial y}\left((\nu + \nu_T)\frac{\partial u}{\partial y}\right), \\ 0 &= -\frac{\partial p}{\partial y}. \end{aligned} \tag{3.100}$$

For axisymmetric flows, we follow the above steps, except starting with the Navier-Stokes equations in cylindrical coordinates (r, θ, z). The corresponding the time-averaged velocities are (U_r, U_θ, W). Since the flow is axisymmetric, we ignore all derivatives in θ and we assume zero swirl ($U_\theta = 0$). The corresponding scalings for the variables are

$$z \sim L, \quad r \sim L\mathrm{Re}^{-1/2}, \quad U_r \sim U_0\mathrm{Re}^{-1/2}, \quad W \sim U_0, \quad P \sim \rho U_0^2. \tag{3.101}$$

Therefore, in dimensional form and reverting the variables back to lower case for convenience, the cylindrical turbulent boundary layer equations are

$$\begin{aligned} \frac{1}{r}\frac{\partial}{\partial r}(ru_r) + \frac{\partial w}{\partial z} &= 0, \\ 0 &= -\frac{1}{\rho}\frac{\partial p}{\partial r}, \\ u_r\frac{\partial w}{\partial r} + w\frac{\partial w}{\partial z} &= -\frac{1}{\rho}\frac{\partial p}{\partial z} + \frac{1}{r}\frac{\partial}{\partial r}\left((\nu + \nu_T)\, r\frac{\partial w}{\partial r}\right). \end{aligned} \tag{3.102}$$

3.7.3 A mixing layer model for unconfined parallel flows

Mixing layers, where two parallel flows undergo turbulent mixing, are a common feature in convection. For laterally unconfined flows, mixing layers can be described using a simple analytical model, which is derived from the turbulent boundary layer equations and Prandtl mixing length theory. In this section we derive this simple model in the absence of buoyancy (i.e. where the flow is momentum-driven rather than density-driven). However, the components of this model will be used later in Section 3.8 when considering convective plumes.

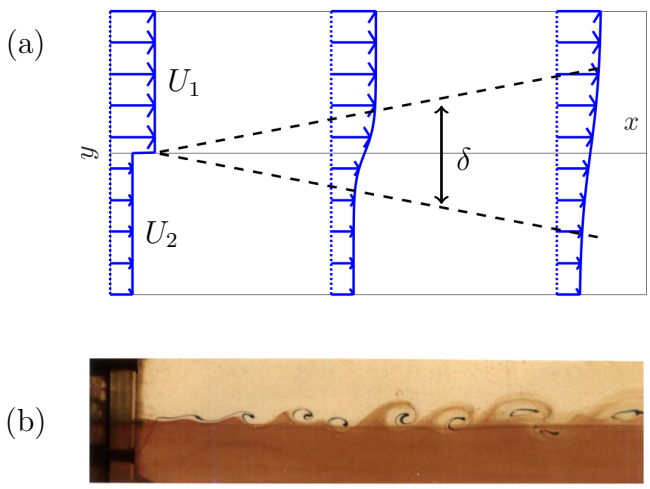

Figure 3.15: (a) Schematic diagram of a mixing layer between parallel flows. (b) Kelvin-Helmholtz vortices in a mixing layer experiment (taken from Lasheras and Choi (1988)).

The flow situation we consider is illustrated in Figure 3.15, in which we illustrate our chosen coordinate system (x, y). A flow with velocity U_1 in the x direction meets a second, parallel flow with velocity $U_2 < U_1$. Due to the Kelvin-Helmholtz instability, the flow profile is unstable to perturbations. The discontinuous jump in velocity between U_2 and U_1 generates a vortex sheet which rolls up downstream into discrete vortical structures. These structures pair and merge forming larger vortical structures. In this way a region of flow forms between the parallel flows which undergoes intense mixing, and which grows downstream, entraining fluid from either side. The time-averaged velocity in the layer is a smoothed quasi-linear profile which increases from U_2 to U_1 over an approximate width $\delta(x)$. The layer is known as a *mixing layer* due to the intense mixing.

The mixing layer region is long and thin, such that the two-dimensional boundary layer approximation applies (3.100). However, since the flow is unconfined it is expected that pressure gradients in the x direction are negligible. Furthermore, we ignore the viscous stress term in (3.100) since we expect $\nu \ll \nu_T$ within the mixing layer. Therefore, the governing equations, defined for $0 \leq x < \infty$ and $-\infty < y < \infty$, are

$$\begin{aligned} \frac{\partial u}{\partial x} + \frac{\partial v}{\partial y} &= 0, \\ u\frac{\partial u}{\partial x} + v\frac{\partial u}{\partial y} &= \frac{\partial}{\partial y}\left(\nu_T \frac{\partial u}{\partial y}\right). \end{aligned} \tag{3.103}$$

The boundary conditions for the streamwise velocity u correspond to matching with

the free stream velocities

$$u(x,\infty) = U_1,$$
$$u(x,-\infty) = U_2, \tag{3.104}$$

and the inflow condition

$$u(0,y) = U_c + \frac{\Delta U}{2}\mathrm{sgn}(y), \tag{3.105}$$

where $U_c = (U_1 + U_2)/2$ is the average velocity and $\Delta U = U_1 - U_2$ is the velocity difference. We also need a boundary condition for v, but we leave this for later discussion.

We rewrite the velocity u in terms of a similarity variable $\zeta = y/\delta(x)$ that depends on the width of the mixing layer, such that

$$u = U_c + \Delta U \frac{\mathrm{d}\mathcal{U}}{\mathrm{d}\zeta}, \tag{3.106}$$

where $\mathcal{U} = \mathcal{U}(\zeta)$ is an unknown function. From (3.103) the transverse velocity v must take the form

$$v = \Delta U \frac{\mathrm{d}\delta}{\mathrm{d}x}\left(\zeta\frac{\mathrm{d}\mathcal{U}}{\mathrm{d}\zeta} - \mathcal{U}\right). \tag{3.107}$$

We use the Prandtl mixing length model (3.98) for the eddy viscosity, where we approximate the velocity gradient by

$$\left|\frac{\partial u}{\partial y}\right| \approx \frac{\Delta U}{\delta}, \tag{3.108}$$

and we use a mixing length proportional to the width of the mixing layer $\ell = C\delta$, such that

$$\nu_T = C^2\delta\Delta U. \tag{3.109}$$

Inserting (3.106), (3.107) and (3.109) into the momentum equation (3.103), we get

$$\frac{\mathrm{d}\delta}{\mathrm{d}x}\frac{U_c}{\Delta U}\left(\frac{\Delta U}{U_c}\mathcal{U} + \zeta\right)\frac{\mathrm{d}^2\mathcal{U}}{\mathrm{d}\zeta^2} + C^2\frac{\mathrm{d}^3\mathcal{U}}{\mathrm{d}\zeta^3} = 0. \tag{3.110}$$

Similarity solutions to (3.110) are only possible if

$$\frac{\mathrm{d}\delta}{\mathrm{d}x}\frac{U_c}{\Delta U} = S, \tag{3.111}$$

where S is a constant known as the spreading parameter, and whose value has been determined by experiments, finding $S = 0.06 - 0.11$. Equation (3.111) is often written in terms of the free stream velocities U_1 and U_2, such that

$$\frac{\mathrm{d}\delta}{\mathrm{d}x} = 2S\frac{U_1 - U_2}{U_1 + U_2}. \tag{3.112}$$

The mixing layer growth rate (3.112) increases with velocity difference, indicating that more non-uniform mixing layers entrain fluid faster.

We simplify (3.110) by introducing rescaled variables

$$\xi = \frac{\sqrt{S}}{C}\zeta, \quad F(\xi) = \frac{\Delta U\sqrt{S}}{U_c C}\mathcal{U}\left(\frac{C\xi}{\sqrt{S}}\right). \tag{3.113}$$

In terms of these new variables (3.110) becomes

$$(\xi + F)\frac{\mathrm{d}^2F}{\mathrm{d}\xi^2} + \frac{\mathrm{d}^3F}{\mathrm{d}\xi^3} = 0, \tag{3.114}$$

and the boundary condition (3.104) becomes

$$\frac{\mathrm{d}F}{\mathrm{d}\xi}(\pm\infty) = \pm\gamma, \tag{3.115}$$

where $\gamma = (U_1 - U_2)/(U_1 + U_2)$.

In the case of a weak mixing layer $\gamma \ll 1$, we rescale $F \sim \gamma$ and the governing equations and boundary conditions simplify to

$$\begin{aligned} \xi\frac{\mathrm{d}^2F}{\mathrm{d}\xi^2} + \frac{\mathrm{d}^3F}{\mathrm{d}\xi^3} &= 0, \\ \frac{\mathrm{d}F}{\mathrm{d}\xi}(\pm\infty) &= \pm 1. \end{aligned} \tag{3.116}$$

This system can be solved explicitly, such that

$$\begin{aligned} \frac{\mathrm{d}F}{\mathrm{d}\xi} &= \mathrm{erf}\,(\xi/\sqrt{2}), \\ F &= \sqrt{2/\pi}e^{-\xi^2/2} + \xi\mathrm{erf}\,(\xi/\sqrt{2}) + D, \end{aligned} \tag{3.117}$$

where D is a constant of integration. This is determined by considering the transverse velocity

$$\lim_{\xi\to\infty}\left(\xi\frac{\mathrm{d}F}{\mathrm{d}\xi} - F\right) = -D = \lim_{\xi\to-\infty}\left(\xi\frac{\mathrm{d}F}{\mathrm{d}\xi} - F\right). \tag{3.118}$$

Hence, we set $D = 0$ to avoid a net mean transverse flow (which is unphysical).

In the case where γ is not small, the transverse boundary condition requires more careful attention. Schlichting (1960) suggested the boundary condition

$$v(x,\infty) = -\frac{U_2}{U_1}v(x,-\infty), \tag{3.119}$$

which is based on a global momentum balance. The condition (3.119) indicates that there is greater entrainment from the slower stream than the faster stream. Hence the dividing streamline, along which $v = 0$, is inclined downwards from the x-axis.

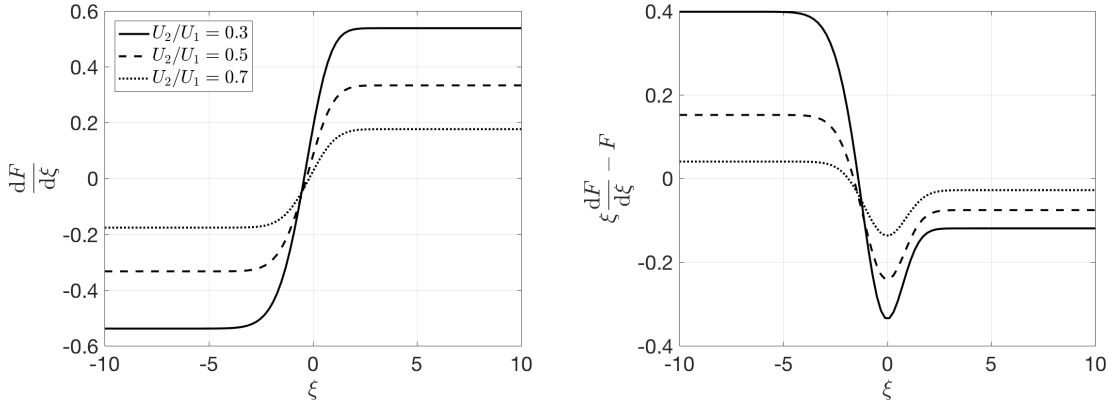

Figure 3.16: Solution to (3.114) for different values of U_2/U_1. (a) Streamwise velocity (3.106) (rescaled). (b) Transverse velocity (3.107) (rescaled).

This is in accordance with experimental observations. In dimensionless terms, this takes the form

$$\lim_{\xi\to\infty}\left(\xi\frac{\mathrm{d}F}{\mathrm{d}\xi} - F\right) = -\left(\frac{U_2}{U_1}\right)\lim_{\xi\to-\infty}\left(\xi\frac{\mathrm{d}F}{\mathrm{d}\xi} - F\right). \tag{3.120}$$

Given a value for U_2/U_1, or equivalently γ, we can solve Equation (3.114), with boundary conditions (3.115) & (3.120), for the function $F(\xi)$. In Figure 3.16 the numerical solution is plotted using three different values of $U_2/U_1 = 0.3, 0.5, 0.7$ (corresponding to $\gamma = 1.08, 0.67, 0.35$).

We can see that the streamwise velocity (a) within the mixing layer is approximately linear. The transverse velocity (b) indicates that there is greater entrainment when the velocity difference is larger, which is consistent with (3.112). However, entrainment is always greater (in magnitude) at the slower stream.

3.8 Parameterised convection

The boundary layer theory described in section 3.5 applies to steady state solutions at high Rayleigh number, but in fact real convection becomes time-varying at such parameter values. The behaviour becomes first oscillatory, and then becomes increasingly irregular, so that at very high Rayleigh numbers, the cellular structure of convection in a fluid layer breaks down. The upwelling and downwelling plumes of the boundary layer theory still exist, but their detachment is sporadic and irregular. In these circumstances, the theoretical description of convection may become, paradoxically, easier. Just as for turbulent shear flows at high Reynolds numbers, one uses empirically-based measures of the fluxes at boundaries to describe the flow. Turbulence mixes the fluid, so that, as in the boundary layer theory, the interior of a convecting cell is taken to be isothermal. In this section, we describe one particular

Figure 3.17: On the left, a sub-oceanic black smoker issuing from a vent at the ocean floor; image from `http://oceanexplorer.noaa.gov`. On the right, a laboratory plume; image courtesy of Andy Woods.

example of turbulent convection to illustrate these ideas. The example is that of the turbulent convective plume.

3.8.1 Plumes

A plume is an isolated convective upwelling. Examples are the rise of smoke from an industrial chimney, the formation of cumulus clouds over oceans, 'black smokers' at mid-ocean rise vents, and explosive volcanic eruptions. In these examples, a source of buoyancy at (essentially) a point drives a convective flow in the fluid above. As suggested in figure 3.17, the plume forms a turbulent, approximately conical region, with a fairly sharp (but time-varying) boundary. The turbulence causes rapid convective mixing, and allows us to conceptualise the plume as a relatively homogeneous cloud of density $\rho = \rho_0 - \Delta\rho$ rising through an ambient medium of density ρ_0. If ρ_0 depends on height z, then the medium is called a stratified medium, and it is stably stratified if $\rho_0'(z) < 0$.

Mathematical model

The simplest mathematical model is of a steady[5] cylindrically symmetric plume of radius $r = b(z)$, in which we use cylindrical coordinates (r, z), with corresponding velocity components (u, w) (thus the upwards fluid velocity is w). The plume rises through a medium of density $\rho_0(z)$. We will make the Boussinesq approximation, which is that variations in density are neglected, except in the buoyancy term of the momentum equation, and in the 'buoyancy' equation itself. This requires variations of the density from that of the ambient density to be small, and also that the variation of ρ_0 with height (if any) is small. We also make the assumption that the plume has a long and thin aspect ratio, such that the boundary layer approximation (3.102) applies. The basic model is then given by

$$\begin{aligned} \frac{1}{r}(ru)_r + w_z &= 0, \\ 0 &= -\frac{1}{\rho_0}p_r, \\ uw_r + ww_z &= -\frac{1}{\rho_0}p_z - \frac{\rho}{\rho_0}g + \frac{1}{r}\frac{\partial}{\partial r}\left[\nu_T r\frac{\partial w}{\partial r}\right], \\ u\rho_r + w\rho_z &= +\frac{1}{r}\frac{\partial}{\partial r}\left[\nu_T r\frac{\partial \rho}{\partial r}\right]. \end{aligned} \tag{3.121}$$

These equations represent respectively conservation of mass, momentum (horizontal and vertical), and buoyancy; p is the pressure, ρ the density, ρ_0 the reference density, and g is the acceleration due to gravity. We have included radial diffusion terms which represent the effects of turbulent mixing. We define the density deficit $\Delta\rho$ in the plume to be

$$\Delta\rho = \rho_0 - \rho. \tag{3.122}$$

The Boussinesq approximation is based on the assumption that $\Delta\rho$ is small, $\Delta\rho \ll \rho_0$.

The rather odd-looking final equation in (3.121) requires some comment. It caters for the fact that the density deficit in plumes may arise because of temperature, dissolved concentrations or particulate load, or a combination. But in all such cases, the turbulent conservation field for the relevant variable is simply that advection is zero; for example we would have $T_t + \mathbf{u}.\boldsymbol{\nabla}T = \boldsymbol{\nabla}.[\nu_T\boldsymbol{\nabla}T]$ for temperature, and similarly for particulate or solute concentrations. Thus the buoyancy conservation equation simply represents this fact, together with the assumption that the density is an algebraic function of the conserved quantities. In certain circumstance, the veracity of this assumption may need to be examined further. For example, in a volcanic ash-laden plume, the eruption column has a density which is dependent on both temperature and ash concentration, and it rises through a surrounding stratified atmosphere whose stratification is itself determined by the relation of density to temperature and pressure. In such circumstance, $(3.121)_4$ may warrant further consideration, but such issues will be ignored here.

[5]The turbulent time variation is averaged out.

The boundary layer approximation implies that radial pressure gradients are negligible, and hence that the pressure is that of the surrounding ambient fluid,

$$p_z \approx -\rho_0 g. \tag{3.123}$$

This allows us to write the remaining three equations in terms of the *reduced gravity*, which is defined to be

$$g' = \frac{g\Delta\rho}{\rho_0}. \tag{3.124}$$

The equations (3.121) then take the simple form

$$\begin{aligned} (ru)_r + rw_z &= 0, \\ uw_r + ww_z &= g' + \frac{1}{r}\frac{\partial}{\partial r}\left[\nu_T r \frac{\partial w}{\partial r}\right], \\ N^2 w + ug'_r + wg'_z &= \frac{1}{r}\frac{\partial}{\partial r}\left[\nu_T r \frac{\partial g'}{\partial r}\right], \end{aligned} \tag{3.125}$$

where N is the Brunt-Väisälä frequency, defined as

$$N = \left(-\frac{g\rho'_0}{\rho_0}\right)^{1/2}, \tag{3.126}$$

and we have put a pre-factor of $1 - \dfrac{\Delta\rho}{\rho_0}$ equal to one in the N^2 term.

It is fairly evident in figure 3.17 that the plume has a fairly well-defined edge, and we will assume this. The boundary of the plume is taken to be at $r = b(z)$. The question then arises as to what, if any, boundary conditions should be applied there. Since the ambient fluid outside the plume has $w = g' = 0$, these are natural conditions to apply, at least when the diffusion terms are included. We therefore pose the conditions

$$w = g' = 0 \quad \text{at} \quad r = b(z). \tag{3.127}$$

One might suppose that also $u = 0$ would be appropriate, but in fact this is found not to be the case. The turbulent eddies of the plume incorporate the ambient fluid, and dramatically increase the plume volume flux. If the entrainment velocity (inwards) at the edge of the plume is u_e, then we have that

$$u = -u_e \quad \text{at} \quad r = b. \tag{3.128}$$

The entrainment velocity needs to be constituted, and a common assumption is to suppose that

$$u_e = \alpha\bar{w}, \tag{3.129}$$

where $\bar{w}$ is the cross-sectionally averaged vertical velocity, and the value of α is found experimentally to be approximately 0.1. We note that the plume boundary $r = b(z)$ is indeterminate, so that an extra condition to determine it is apparently necessary. If $b = \infty$, this issue does not arise.

The case $\nu_T = 0$

We now ignore the radial diffusion terms in (3.125) by putting $\nu_T = 0$. The resulting equations are given by

$$\begin{aligned} (ru)_r + rw_z &= 0, \\ uw_r + ww_z &= g', \\ ug'_r + wg'_z &= -N^2 w, \end{aligned} \tag{3.130}$$

and are hyperbolic, and suitable boundary conditions to consider are (3.127) and (3.128) at the plume boundary; in addition, for a plume emanating from a vent of radius a at $z = 0$, we might pose

$$w = w_0, \quad u = 0, \quad g' = g'_0 \quad \text{at} \quad z = 0, \quad 0 < r < a. \tag{3.131}$$

Whether all these conditions can be applied depends on the characteristic directions of the hyperbolic set (3.130). This is examined in question 3.8. If we define the Stokes stream function by $ru = \psi_z$, $rw = -\psi_r$, then the characteristics are just the streamlines, and follow the direction of flow. Therefore the characteristics point inwards from all parts of the boundary, and all the boundary conditions can be applied.

Without writing an analytical solution for the flow, what happens is fairly clear (we assume positive vent buoyancy, $g'_0 > 0$). On the streamlines from the vent which form the central part of the plume, $g' \equiv g'_0$, and w increases upwards, thus the vent streamlines shrink radially. Equally, the prescription of $g' = 0$ on the plume boundary $r = b$ ensures that $g' = w = 0$ on all characteristics that begin there, so that $g' = 0$ everywhere outside the vent characteristics; the characteristics are horizontal. In fact, there is no reason to define the plume outside the central core, since there is no buoyancy there.

It is fairly clear what the matter is: the diffusion terms in (3.125) can not be ignored. Their effect is precisely to broaden the spike of buoyancy which emerges from the vent. We can go further. A typical prescription for the eddy viscosity is to take (in the present situation)

$$\nu_T = \varepsilon_T b w, \tag{3.132}$$

where ε_T is relatively small, perhaps $\sim 10^{-2}$. The point is that with this assumption, the eddy viscosity tends to zero at the plume edge, which suggests as with other examples of such degenerate diffusion that no extra condition is necessary to determine it (and that its location is at a finite distance).

Moment equations

In order to progress with the solution of the equations (3.125), we integrate them from the centre to the edge of the plume, the second and third after multiplying by

r. With our assumption that $\nu_T = 0$ when $w = 0$, the two diffusion integrals vanish, and we are left with three evolution equations for the three quantities

$$\begin{aligned} Q &= 2\pi \int_0^b rw\, dr, \\ M &= 2\pi \int_0^b rw^2\, dr, \\ B &= 2\pi \int_0^b rwg'\, dr, \end{aligned} \tag{3.133}$$

which are the volume flux, the momentum flux and the buoyancy flux, respectively. Bearing in mind that $w = g' = 0$ at $r = b$, we find, noting also (3.128) and (3.129),

$$\begin{aligned} \frac{dQ}{dz} &= 2\pi\alpha b\bar{w}, \\ \frac{dM}{dz} &= 2\pi \int_0^b rg'\, dr, \\ \frac{dB}{dz} &= -N^2 Q. \end{aligned} \tag{3.134}$$

We note also that

$$Q = \pi b^2 \bar{w}, \tag{3.135}$$

so that these are almost self-contained. In order to proceed, some further simplifications must be made. We consider first the case of an unstratified environment.

Unstratified environment

In the case that the ambient fluid is unstratified, the Brunt-Väisälä frequency N is zero, and the buoyancy flux B is constant. In practice it is sufficient to consider the release of buoyant material from a point source, as this effectively is the common situation of interest. If in addition we suppose that the volume flux (and hence also the momentum flux) is zero at the source, then there is no intrinsic length scale in the problem, and a similarity solution is suggested. Indeed, the only dimensional quantities in the problem are the buoyancy flux B with units of $\mathrm{m}^4\ \mathrm{s}^{-3}$ and the lengths r and z. So the similarity variable must be

$$\eta = \frac{r}{z}, \tag{3.136}$$

and the solution must have the form, by dimensional reasoning,

$$b = \beta z, \quad w = B^{1/3} z^{-1/3} W(\eta), \quad g' = B^{2/3} z^{-5/3} G(\eta), \tag{3.137}$$

with u being determined by quadrature. It seems that these expressions fit well to experiments, with the functions W and G being approximately Gaussians.

The question then arises, can we actually find the functions W and G by solving the model (3.125)? As we might expect, the equations without the diffusion terms admit a similarity form of solution, although as discussed above this is of little use. What is (perhaps) surprising is that the equations (3.125) *including* the diffusion terms, have a similarity solution of the form

$$w = z^\nu W(\eta), \quad u = z^\nu U(\eta), \quad g' = z^{2\nu-1}G(\eta), \quad \eta = \frac{r}{z}, \quad b = \beta z, \quad \nu = -\tfrac{1}{3}, \tag{3.138}$$

providing we choose the eddy viscosity to be given by (3.132), and then U, W and G satisfy the equations

$$\begin{aligned} (\eta U)' + \eta(\nu W - \eta W') &= 0, \\ UW' + W(\nu W - \eta W') &= G + \frac{\varepsilon_T \beta}{\eta}(\eta W W')', \\ UG' + W\{(2\nu-1)G - \eta G'\} &= \frac{\varepsilon_T \beta}{\eta}(\eta W G')', \end{aligned} \tag{3.139}$$

with such boundary conditions as we can muster:

$$W = G = 0, \quad U = -\frac{2\alpha}{\beta^2}\int_0^\beta \eta W \, d\eta \quad \text{at} \quad \eta = \beta. \tag{3.140}$$

There will be symmetry conditions at $\eta = 0$, but since the equations in (3.139) are degenerate at both end points (and β is not known), it is unclear just how many conditions are necessary. In addition we have the prescribed buoyancy flux B, which gives another condition via the presumed first integral

$$B = 2\pi \int_0^\beta \eta W G \, d\eta. \tag{3.141}$$

It remains to be seen whether the numerical solution of (3.139) gives solutions similar to observations.

Plumes in a stratified environment

If, as for example in the atmosphere, the ambient density decreases with height, then a similarity solution is no longer feasible because the stratification introduces a natural scale height. To derive a model for such a plume, we must assume some form for the cross-section profiles, which will allow closure expressions for the average fluxes B, Q and M in terms of the plume (average) velocity w and radius b. The simplest assumption to make is that the profiles of buoyancy and vertical velocity have 'top hat' profiles, that is to say they are uniform and then drop rapidly at the plume edges. Such profiles might be motivated by a particular choice of expression for the eddy viscosity in (3.125), for example. With this assumption, we find

$$B = \pi b^2 w g', \quad Q = \pi b^2 w, \quad M = \pi b^2 w^2; \tag{3.142}$$

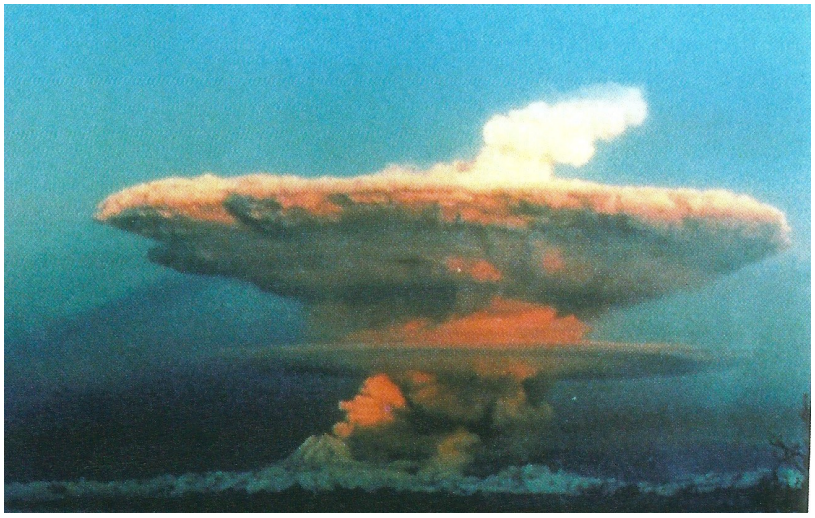

Figure 3.18: An umbrella cloud resulting from the eruption of Mount Redoubt, Alaska, in 1991. Image from Huppert (2000).

in addition we have

$$2\pi \int_0^b rg' \, dr = \pi b^2 g'. \tag{3.143}$$

Eliminating w and b finally yields the equations

$$\begin{aligned} \frac{dB}{dz} &= -N^2 Q, \\ \frac{dM}{dz} &= \frac{BQ}{M}, \\ \frac{dQ}{dz} &= 2\pi^{1/2} \alpha M^{1/2}. \end{aligned} \tag{3.144}$$

We can see from this that the buoyancy flux continually decreases with height, while the volume flux increases. When $B = 0$, the plume reaches its level of neutral buoyancy, but continues to rise because of its momentum. With $B < 0$, M decreases, and will not rise any further when M reaches 0. According to the equations, the volume flux is still positive, but in fact the plume spreads out laterally, forming an *umbrella cloud* as shown in figure 3.18, and the one-dimensional description becomes irrelevant. Thus a plume in a stratified medium will level out at a height z_s which can be determined from (3.144) in the form (see question 3.11)

$$z_s = cB_0^{1/4} N^{-3/4}, \tag{3.145}$$

where B_0 is the buoyancy flux at $z = 0$, and N is assumed constant.

3.9 Turbulent convection

As the Rayleigh number increases in Rayleigh–Bénard convection, the convective rolls which can be seen at the onset of convection bifurcate to three-dimensional planforms, typically either square cells or hexagons. In a layer of large horizontal extent, convective rolls tend to be weakly chaotic, because the alignment in different parts of the layer is different, and thus defects or dislocations are formed in the cellular structure, and these migrate slowly, sometimes permanently. Three-dimensional cells tend to be more stable, because they are essentially confined, but at higher Rayleigh number, an oscillatory instability sets in. The thermal boundary layers which migrate across the base of the cells and detach at the cell boundaries start to prematurely thicken and then thin again before detachment, causing an oscillation which is a manifestation of budding plume development. Eventually, these budding plumes do begin to detach before reaching the cell walls, and at this point the convection becomes temporally and spatially disordered. Thermal boundary layers thicken and plumes detach irregularly, and a defined cellular structure disappears, being replaced by a host of upwelling and downwelling thermal plumes. In fact, a large scale circulation does come into existence, but this is on a much larger scale than the typical plume spacing.

A very famous but simple model of turbulent thermal convection was put forward by Lou Howard in 1964, at the International Congress of Mechanics in Munich. In his model, a quiescent thermal boundary layer grows into an isothermal core until it reaches a critical thickness, when it suddenly forms a plume and detaches, mixing the fluid and returning to isothermal conditions. The average heat flux is then determined by that during the quiescent, conductive phase. The conductive temperature in the growing boundary layer is given by the solution of

$$T_t = \kappa T_{zz}, \tag{3.146}$$

with

$$\begin{aligned} T = \tfrac{1}{2}\Delta T \quad &\text{on} \quad z = 0, \\ T \to 0 \quad &\text{as} \quad z \to \infty; \end{aligned} \tag{3.147}$$

here we imagine a convecting fluid layer of depth d, across which the prescribed temperature difference is ΔT (and thus half across the boundary layers on each surface). Starting from an isothermal state $T = 0$ (boundary layer of thickness zero), the solution is

$$T = \tfrac{1}{2}\Delta T \operatorname{erfc}\left(\frac{z}{2\sqrt{\kappa t}}\right), \tag{3.148}$$

and thus the average heat flux from the surface $z = 0$ is

$$F = \frac{1}{t_c}\int_0^{t_c} \left(-k\frac{\partial T}{\partial z}\right)\bigg|_{z=0} dt, \tag{3.149}$$

where t_c is the time of detachment of the boundary layer. Using (3.148), we then find

$$F = \frac{k\Delta T}{2\sqrt{\kappa t_c}} = \frac{k\Delta T}{2d_c}, \tag{3.150}$$

where $d_c = \sqrt{\kappa t_c}$ is the thickness of the thermal boundary layer at detachment.

Howard hypothesised that detachment would occur when a locally defined Rayleigh number, using the boundary layer thickness as the depth scale, became critical, of order

$$Ra_c \sim 10^3; \tag{3.151}$$

thus we define the critical thickness d_c via the effective critical Rayleigh number condition

$$\frac{\alpha\rho_0 g d_c^3 \Delta T}{2\mu\kappa} = Ra_c, \tag{3.152}$$

where the factor 2 allows for the temperature drop of $\frac{1}{2}\Delta T$ across the boundary layer. In terms of the Rayleigh number of the fluid layer

$$Ra = \frac{\alpha\rho_0 g d^3 \Delta T}{\mu\kappa}, \tag{3.153}$$

we thus have the dimensionless heat flux, called the Nusselt number Nu, given by

$$Nu = \frac{F}{(k\Delta T/d)} = \frac{d}{d_c} = cRa^{1/3}, \tag{3.154}$$

where

$$c = (2Ra_c)^{-1/3} \approx 0.08. \tag{3.155}$$

Thus the heat flux can be parameterised as

$$F = c\left(\frac{\alpha g c_p}{\mu}\right)^{1/3} (\rho_0 k)^{2/3}\, \Delta T^{4/3}, \tag{3.156}$$

which is the famous four-thirds law for turbulent convection. It is reasonably consistent with experimental results.

3.10 Notes and references

The theory of continental drift was famously published by Alfred Wegener, a German meteorologist, in 1915. An English translation of his book was published later, see Wegener (1924). His ideas were scorned by the geophysical establishment, and in particular, in Britain, by the colossal figure of Harold Jeffreys. The blind ignorance with which he and other fellow geologists refuted Wegener's ideas should serve (but have not) as a lesson for scientists against the perils of treating science as religion, and hypothesis as dogma. A notable supporter of the thesis of continental drift was

Holmes (1978), who understood that mantle convection was the driving mechanism. A more modern treatment of geodynamics is the classic book by Turcotte and Schubert (1982), while Davies (1999) gives a readable but technically undemanding account.

The layered magma chamber known as the Skaergaard intrusion was the subject of a massive memoir by Wager and Brown (1968), who gave painstaking descriptions of the series of layered rocks. They made some attempts at a theoretical description, as did McBirney and Noyes (1979), based on analogous processes in chemical reaction-diffusion theory. Neither of these, nor any subsequent attempts at a theoretical model, have been altogether successful.

Baines and Gill (1969), Turner (1979)

Balmforth *et al.* (2001)

The basic description of boundary layer theory at high Rayleigh number and infinite Prandtl number was first done successfully by Turcotte and Oxburgh (1967). A more complete theory is due to Roberts (1979), although even this is not quite watertight.. The necessary numerical results to compute C in (3.37) are given by Roberts (1979) and Jimenez and Zufiria (1987). The results are slightly different, with the latter paper considering Roberts' numerical results to be wrong. For $a = O(1)$, then $2C \approx 0.1$.

Jimenez and Zufiria (1987) claim that the equivalent problem to (3.48) for the case of no-slip boundary conditions has no solution, but do not adduce details. Their inference is that the boundary layer approximation fails: this seems a hazardous conclusion.

Linden (2000), Morton *et al.* (1956).

The model of turbulent thermal convection described in section 3.9 is due to Howard (1966). Baines and Turner (1969).

Exercises

3.1 The Boussinesq equations of two-dimensional thermal convection can be written in the dimensionless form

$$\begin{aligned} \boldsymbol{\nabla}.\mathbf{u} &= 0, \\ \frac{1}{Pr}[\mathbf{u}_t + (\mathbf{u}.\boldsymbol{\nabla})\mathbf{u}] &= -\boldsymbol{\nabla}p + \nabla^2\mathbf{u} + Ra\,T\hat{\mathbf{k}}, \\ T_t + \mathbf{u}.\boldsymbol{\nabla}T &= \nabla^2 T. \end{aligned}$$

Explain the meaning of these equations, and write down appropriate boundary conditions assuming stress-free boundaries.

By introducing a suitably defined stream function, show that these equations can be written in the form

$$\begin{aligned} \frac{1}{Pr}\left[\nabla^2\psi_t + \psi_x\nabla^2\psi_z - \psi_z\nabla^2\psi_x\right] &= Ra\,T_x + \nabla^4\psi, \\ T_t + \psi_x T_z - \psi_z T_x &= \nabla^2 T, \end{aligned}$$

with the associated boundary conditions

$$\begin{aligned} \psi = \nabla^2\psi = 0 \quad &\text{at} \quad z = 0, 1, \\ T = 0 \quad &\text{at} \quad z = 1, \\ T = 1 \quad &\text{at} \quad z = 0, \end{aligned}$$

and write down the conductive steady state solution.

By linearising about this steady state, show that

$$\frac{1}{Pr}\left(\frac{\partial}{\partial t} - \nabla^2\right)\nabla^2\psi_t = \left(\frac{\partial}{\partial t} - \nabla^2\right)\nabla^4\psi + Ra\,\psi_{xx},$$

and deduce that solutions are $\psi = e^{\sigma t}\sin kx \sin m\pi z$, and thus that

$$(\sigma + K^2)\left(\frac{\sigma}{K^2 Pr} + 1\right) - \frac{Ra\,k^2}{K^4} = 0, \quad K^2 = k^2 + m^2\pi^2.$$

By considering the graph of this expression as a function of σ, show that oscillatory instabilities can not occur, and hence derive the critical Rayleigh number for the onset of convection.

3.2 A two-dimensional, incompressible fluid flow has velocity $\mathbf{u} = (u, 0, w)$, and depends only on the coordinates x and z. Show that there is a stream function ψ satisfying $u = -\psi_z$, $w = \psi_x$, and that the vorticity

$$\boldsymbol{\omega} = \boldsymbol{\nabla} \times \mathbf{u} = -\nabla^2\psi\mathbf{j},$$

and thus that

$$\mathbf{u} \times \boldsymbol{\omega} = (\psi_x\nabla^2\psi, 0, \psi_z\nabla^2\psi),$$

and hence

$$\boldsymbol{\nabla} \times (\mathbf{u} \times \boldsymbol{\omega}) = (\psi_x\nabla^2\psi_z - \psi_z\nabla^2\psi_x)\mathbf{j}.$$

Use the vector identity $(\mathbf{u}.\boldsymbol{\nabla})\mathbf{u} = \boldsymbol{\nabla}(\frac{1}{2}u^2) - \mathbf{u} \times \boldsymbol{\omega}$ to show that

$$\boldsymbol{\nabla} \times \frac{d\mathbf{u}}{dt} = \left[-\nabla^2\psi_t - \psi_x\nabla^2\psi_z + \psi_z\nabla^2\psi_x\right]\mathbf{j}.$$

Show also that

$$\boldsymbol{\nabla} \times \theta\mathbf{k} = -\theta_x\mathbf{j},$$

and use the Cartesian identity

$$\nabla^2 \equiv \text{grad}\,\text{div} - \text{curl}\,\text{curl}$$

to show that

$$\boldsymbol{\nabla} \times \nabla^2\mathbf{u} = -\nabla^4\psi\,\mathbf{j},$$

and hence deduce that the momentum equation for Rayleigh–Bénard convection can be written in the form

$$\frac{1}{Pr}\left[\nabla^2\psi_t + \psi_x\nabla^2\psi_z - \psi_z\nabla^2\psi_x\right] = Ra\,\theta_x + \nabla^4\psi.$$

3.3 Suppose that σ satisfies

$$p(\sigma) \equiv \sigma^3 + a\sigma^2 + b\sigma + c = 0,$$

and that a, b and c are positive. Suppose, firstly, that the roots are all real. Show in this case that they are all negative.

Now suppose that one root (α) is real and the other two are complex conjugates $\beta \pm i\gamma$. Show that $\alpha < 0$. Show also that $\beta < 0$ if $a > \alpha$. Show that $a > \alpha$ if $p(-a) < 0$, and hence show that $\beta < 0$ if $c < ab$.

If

$$\begin{aligned} a &= K^2\left(Pr + 1 + \frac{1}{Le}\right), \\ b &= K^4\left(Pr + \frac{1}{Le} + \frac{Pr}{Le}\right) + \frac{k^2}{K^2}Pr(Rs - Ra), \\ c &= \frac{K^6}{Le}Pr + k^2 Pr\left(Rs - \frac{Ra}{Le}\right), \end{aligned}$$

show that $a, b, c > 0$ if $Ra < 0$, $Rs > 0$, and show that if $Le > 1$, then $c < ab$.

What does this tell you about the stability of a layer of fluid which is both thermally and salinely stably stratified?

3.4 Suppose that σ satisfies

$$p(\sigma) \equiv \sigma^3 + a\sigma^2 + b\sigma + c = 0,$$

and that all the roots have negative real part if $c < ab$. Show that the condition that there be two purely imaginary roots $\pm i\Omega$ is that $c = ab$, and deduce that there are two (complex) roots with positive real part if $c > ab$. With

$$\begin{aligned} a &= K^2\left(Pr + 1 + \frac{1}{Le}\right), \\ b &= K^4\left(Pr + \frac{1}{Le} + \frac{Pr}{Le}\right) + \frac{k^2}{K^2}Pr(Rs - Ra), \\ c &= \frac{K^6}{Le}Pr + k^2 Pr\left(Rs - \frac{Ra}{Le}\right), \end{aligned}$$

show that this condition reduces to

$$Ra > \frac{\left(Pr + \frac{1}{Le}\right)Rs}{1 + Pr} + \frac{\left(1 + \frac{1}{Le}\right)\left(Pr + \frac{1}{Le}\right)}{Pr}\frac{K^6}{k^2}.$$

Assuming $K^2 = k^2 + m^2\pi^2$, where m is an integer, show that the minimum value of Ra where this condition is satisfied is when $m = 1$, and give the corresponding critical value $Ra_{\rm osc}$.

3.5 On the line XV in figure 3.9, the cubic

$$p(\sigma) = \sigma^3 + a\sigma^2 + b\sigma + c$$

has two positive real roots β and one negative real root α. Show that the condition for this to be the case is that

$$a = \alpha - 2\beta, \quad b = \beta^2 - 2\alpha\beta, \quad c = \alpha\beta^2,$$

and deduce that

$$a\beta^2 + 2b\beta + 3c = 0. \quad (1)$$

Show also that at the double root β,

$$3\beta^2 + 2a\beta + b = 0. \quad (2)$$

Deduce from (1) and (2) that

$$\beta = \frac{9c - ab}{a^2 - 6b},$$

and hence, using (2), that

$$\beta = \tfrac{1}{3}\left[-a + \{a^2 - 3b\}^{1/2}\right]. \quad (3)$$

Explain why the positive root is taken in (3), and why we can assume $b < 0$.

Use the definitions

$$\begin{aligned} a &= K^2\left(Pr + 1 + \frac{1}{Le}\right), \\ b &= K^4\left(Pr + \frac{1}{Le} + \frac{Pr}{Le}\right) + \frac{k^2}{K^2}Pr(Rs - Ra), \\ c &= \frac{K^6}{Le}Pr + k^2 Pr\left(Rs - \frac{Ra}{Le}\right), \end{aligned}$$

to show that if $Ra \sim Rs \gg 1$, $Ra - Rs \gg 1$ and $Le \gg 1$, then XV is approximately given by

$$Ra \approx Rs + \frac{3K^2 Rs^{2/3}}{(4k^2 Pr)^{2/3}}.$$

3.6 The growth rate σ for finger instabilities is given by

$$(\sigma + K^2 Pr)(\sigma + K^2)\left(\sigma + \frac{K^2}{Le}\right) + k^2 Pr\left[\frac{(Rs - Ra)\sigma}{K^2} + Rs - \frac{Ra}{Le}\right] = 0,$$

and $Ra, Rs < 0$ with $-Ra, -Rs \gg 1$; K is defined by $K^2 = k^2 + \pi^2$.

Define $Rs = Ra\, r$, and consider the behaviour of the roots when $Ra \to -\infty$ with r fixed. Show that when k is $O(1)$, one root is given by

$$\sigma = \frac{\left(r - \dfrac{1}{Le}\right) K^2}{1 - r} + O\left(\frac{1}{|Ra|}\right), \quad (*)$$

and that this is positive if

$$\frac{1}{Le} < r < 1.$$

Show that the other two roots are of $O\left(|Ra|^{1/2}\right)$, and by putting

$$\sigma = |Ra|^{1/2}\Sigma_0 + \Sigma_1 + \ldots,$$

show that they are given by

$$\sigma = \pm i\frac{k}{K}\{Pr(Ra - Rs)\}^{1/2} - \tfrac{1}{2}K^2\left(Pr + \frac{1 - \dfrac{1}{Le}}{1 - r}\right) + O\left(\frac{1}{|Ra|^{1/2}}\right),$$

and thus represent stable modes.

Show further that when k is large, an appropriate scaling when $(*)$ breaks down is given by

$$k = |Ra|^{1/4}\alpha, \quad \sigma = |Ra|^{1/2}\Sigma,$$

and write down the equation satisfied by Σ in this case. Show also that when α is large, the three roots are all negative, with $\Sigma \sim -\alpha^2 S$, and $S = Pr$, 1, or $\dfrac{1}{Le}$.

Deduce that the maximal growth rate for finger instability occurs when $k \sim |Ra|^{1/4}$.

3.7 The scaled Boussinesq equations for two-dimensional thermal convection at infinite Prandtl number and large Rayleigh number R in $0 < x < a$, $0 < z < 1$, can be written in the form

$$\omega = -\nabla^2\psi,$$

$$\nabla^2\omega = \frac{1}{\delta}T_x,$$

$$\psi_x T_z - \psi_z T_x = \delta^2\nabla^2 T,$$

where $\delta = R^{-1/3}$. Explain what is meant by the Boussinesq approximation, and explain what the equations represent. Explain why suitable boundary conditions for these equations which represent convection in a box with stress free boundaries, as appropriate to convection in the Earth's mantle, are given by

$$\psi = 0, \quad \omega = 0, \quad \text{on} \quad x = 0,\ a, \quad z = 0,\ 1,$$

$$T = \tfrac{1}{2} \quad \text{on} \quad z = 0, \quad T = -\tfrac{1}{2} \quad \text{on} \quad z = 1, \quad T_x = 0 \quad \text{on} \quad x = 0, \ a.$$

Show that, if $\delta \ll 1$, there is an interior 'core' in which $T \approx 0$, $\nabla^4 \psi = 0$.

By writing $1 - z = \delta Z$, $\psi = \delta \Psi$ and $\omega = \delta \Omega$, show that $\Psi \approx u_s(x) Z$, and deduce that the temperature in the thermal boundary layer at the surface is described by the approximate equation

$$u_s T_x - Z u_s' T_Z \approx T_{ZZ},$$

with

$$T = -\tfrac{1}{2} \quad \text{on} \quad Z = 0, \quad T \to 0 \quad \text{as} \quad Z \to \infty.$$

If u_s is constant, find a similarity solution, and show that the scaled surface heat flux $q = \partial T / \partial Z|_{Z=0}$ is given by

$$q = \frac{1}{2} \sqrt{\frac{u_s}{\pi x}}.$$

3.8 The Boussinesq equations describing the rise of a cylindrical plume are, ignoring turbulent eddy viscosity,

$$\begin{aligned} (ru)_r + r w_z &= 0, \\ u w_r + w w_z &= g', \\ u g_r' + w g_z' &= 0, \end{aligned}$$

in which r and z are cylindrical coordinates, u and w are radial and vertical velocities, and g' is the reduced gravity. Explain the basis for the derivation of these equations, including a definition of what is meant by the 'reduced gravity'.

Write the equations in the form

$$A \boldsymbol{\phi}_r + B \boldsymbol{\phi}_z = \mathbf{c},$$

and hence show that the characteristics $\dfrac{dr}{dz} = \lambda$ satisfying $\det(A - \lambda B) = 0$ are

$$\lambda = \frac{u}{w}, \ \frac{u}{w}, \ \infty.$$

What is meant by saying that the third characteristic is ∞? What might make it finite?

Define a suitable stream function ψ for the flow, and show that the characteristics are the streamlines.

Assuming the plume emerges from a chimney of finite radius a with uniform upwards speed w_0 and uniform buoyancy (reduced gravity) $g_0 > 0$, and that entrainment occurs at the plume edge, write down suitable boundary conditions

for the flow, and draw a sketch of the resulting characteristic diagram. (Assume that the plume boundary $b(z) > a$.)

By explicitly solving the characteristic equations, show that the edge of the central part of the plume is given by

$$r = \frac{a}{\left(1 + \dfrac{2g_0 z}{w_0^2}\right)^{1/4}}.$$

What happens if $g_0 < 0$? Explain this physically.

3.9 The equations describing the steady motion of a turbulent plume in $z > 0$ and $0 < r < b(z)$ (using cylindrical polar coordinates) are

$$\begin{aligned}
(ru)_r + rw_z &= 0, \\
uw_r + ww_z &= g' + \frac{1}{r}\frac{\partial}{\partial r}\left[\nu_T r \frac{\partial w}{\partial r}\right], \\
N^2 w + ug'_r + wg'_z &= \frac{1}{r}\frac{\partial}{\partial r}\left[\nu_T r \frac{\partial g'}{\partial r}\right],
\end{aligned}$$

where u and w are radial and vertical velocities, g' is the reduced gravity, N is the Brunt–Väisälä frequency, and the eddy viscosity is assumed to be

$$\nu_T = \varepsilon_T b w,$$

where $\varepsilon_T \ll 1$. Boundary conditions for the flow are

$$w = g' = 0, \quad u = -\alpha \bar{w} \quad \text{at} \quad r = b,$$

where $\bar{w}$ is the cross-sectional average of w and α (≈ 0.1) is a positive constant, and

$$w = w_0, \quad g' = g_0 \equiv \frac{g\Delta\rho}{\rho_0} \quad \text{at} \quad z = 0, 0 < r < a,$$

where also $b(0) = a$.

Assuming a stratified atmosphere in which $-\dfrac{1}{\rho_0}\dfrac{\partial \rho_0}{\partial z} \sim \dfrac{1}{H}$ (H is the scale height) and that $w_0 \lesssim \sqrt{g_0 l}$, show how to non-dimensionalise the equations so that all the terms in each equation balance. Hence show that the plume aspect ratio is ε_T, and that the natural length scale is $l \sim \dfrac{H\Delta\rho}{\rho_0}$.

By defining a stream function ψ with $\psi = 0$ on $r = 0$ and $\psi > 0$ for $r > 0$, make a Von Mises transformation from variables z, r to z, ψ, and hence show that w and g' satisfy nonlinear diffusion-type equations.

3.10 An isolated turbulent cylindrical plume in a stratified medium of density $\rho_0(z)$ is described by the inviscid Boussinesq equations

$$uu_r + wu_z = -\frac{1}{\rho_0}p_r,$$

$$uw_r + ww_z = -\frac{1}{\rho_0}p_z - \frac{\rho}{\rho_0}g,$$

$$u\rho_r + w\rho_z = 0,$$

$$\frac{1}{r}(ru)_r + w_z = 0,$$

where (r, z) are cylindrical coordinates, (u, w) the corresponding velocity components, p the pressure, ρ the density, ρ_0 the reference density, and g is the acceleration due to gravity. If $\rho = \rho_0 - \Delta\rho$, explain what is meant by the Boussinesq approximation.

Suppose the edge of the plume is at radius $r = b$, such that $w = 0$ there. Suppose also that the plume entrains ambient fluid, such that

$$(ru)|_b = -b\alpha\bar{w},$$

where $\bar{w}$ denotes the cross-sectional average value of w. Deduce that the plume volume flux

$$Q = 2\pi \int_0^b rw\, dr$$

satisfies

$$\frac{dQ}{dz} = 2\pi\alpha b\bar{w}.$$

The momentum flux is defined by

$$M = 2\pi \int_0^b rw^2\, dr.$$

Show that, assuming that

$$\frac{\partial p}{\partial z} = -\rho_0 g$$

throughout the plume, that

$$\frac{dM}{dz} = 2\pi \int_0^b rg'\, dr,$$

where

$$g' = \frac{g\Delta\rho}{\rho_0}.$$

Why would the hydrostatic approximation be appropriate?

The buoyancy flux is defined by

$$B = 2\pi \int_0^b rwg' \, dr;$$

assuming $g' = 0$ at $r = b$, show that

$$\frac{dB}{dz} = -N^2 Q,$$

where the Brunt–Väisälä frequency N is defined by

$$N = \left(-\frac{g\rho_0'(z)}{\rho_0} \right)^{1/2}.$$

3.11 The buoyancy flux B, momentum flux M, and mass flux Q of a turbulent plume in a stratified atmosphere satisfy the equations

$$\frac{dB}{dz} = -N^2 Q,$$

$$\frac{dM}{dz} = 2\pi \int_0^b rg' \, dr,$$

$$\frac{dQ}{dz} = 2\pi\alpha b w,$$

where w is the plume velocity, b is its radius, g' is the reduced gravity, N is the Brunt–Väisälä frequency, $\alpha \approx 0.1$ is an entrainment coefficient, and r and z are radial and axial coordinates. Assuming that

$$2\pi \int_0^b rA \, dr = \pi b^2 A$$

for any plume quantity, assumed to be approximated by a top hat profile, show that

$$\frac{dB}{dz} = -N^2 Q,$$

$$\frac{dM}{dz} = \frac{BQ}{M},$$

$$\frac{dQ}{dz} = 2\pi^{1/2}\alpha M^{1/2}.$$

Now suppose that $B = B_0$, $M = Q = 0$ at $z = 0$. By non-dimensionalising the equations appropriately, show that the level of neutral buoyancy where $B = 0$ is given by

$$z_s = \frac{\zeta_s}{(2\alpha\pi^{1/2})^{1/2}} \frac{B_0^{1/4}}{N^{3/4}},$$

where ζ_s is a numerical constant (it is approximately measured to be 1.5). Write down the equations and boundary conditions necessary to determine ζ_s, and by integrating them, show that

$$\zeta_s = \int_0^1 \frac{db}{\left[2\int_b^1 (1-\beta^2)^{1/4}\, d\beta\right]^{1/2}}.$$

If, instead, $w = w_0$ and $b = b_0$ at $z = 0$, show that the same model to determine z_s is valid provided w_0 and b_0 are small enough, and specifically if

$$w_0 \ll \frac{g'}{N}, \quad b_0^2 w_0 \ll \frac{g'^3}{N^5}.$$

Show that if the first inequality is satisfied, then the second is as well, provided

$$b_0 \lesssim \frac{g'}{N^2}.$$

If the scale height of the medium is h (i. e., $\rho_0'/\rho \sim 1/h$), show that these two inequalities take the form

$$w_0 \ll \frac{\Delta\rho}{\rho_0}\sqrt{gh}, \quad b_0 \lesssim \frac{\Delta\rho}{\rho_0} h.$$

References

Baines, P. G. and A. E. Gill 1969 On thermohaline convection with linear gradients. J. Fluid Mech. **37**, 289-306.

Baines, W. D. and J. S. Turner 1969 Turbulent buoyant convection from a source in a confined region. J. Fluid Mech. **37**, 51-80.

Balmforth, N. J., A. Provenzale and J. A. Whitehead 2001 The language of pattern and form. In: Geomorphological fluid mechanics, eds. N. J. Balmforth and A. Provenzale, pp. 3-33. Springer-Verlag, Berlin.

Barlow, P. M. 2003. Ground water in freshwater-saltwater environments of the Atlantic coast (Vol. 1262). Washington, DC, USA: US Department of the Interior, US Geological Survey.

Batchelor, G. K. 1967 An introduction to fluid dynamics. C. U. P., Cambridge.

Benham, G.P., 2018. Mathematical modelling and optimisation of Venturi-enhanced hydropower (Doctoral dissertation, University of Oxford).

Benney, D., 1966 Long waves on liquid films. J Math. and Phy., **45**(1-4), pp.150-155.

Bui, M., Adjiman, C.S., Bardow, A., Anthony, E.J., Boston, A., Brown, S., Fennell, P.S., Fuss, S., Galindo, A., Hackett, L.A. and Hallett, J.P., 2018. Carbon capture and storage (CCS): the way forward. Energy & Environmental Science, 11(5), pp.1062-1176.

Davies, G. F. 1999 Dynamic Earth: plates, plumes and mantle convection. C. U. P., Cambridge.

Dubs, W. 1939 Uber den einfluß laminarer und turbulenter strömung auf das röntgenbild von wasser und nitrobenzol. Ein röntgenographischer Beitrag zum Turbulenzproblem. Helv. phys. Acte, 12, pp.169-228.

Holmes, A. 1978 Principles of physical geology. 3rd edition, revised by Doris Holmes. John Wiley and sons, New York.

Howard, L. N. 1966 Convection at high Rayleigh number. Proc. 11th Int. Cong. Appl. Mech., ed. H. Görtler, pp. 1109-1115. Springer, Berlin.

Huppert, H. E. 2000 Geological fluid mechanics. In: Batchelor, G. K., H. K. Moffatt and M. G. Worster (eds.), Perspectives in fluid dynamics, pp. 447-506. C. U. P., Cambridge.

Jimenez, J. and J. A. Zufiria 1987 A boundary layer analysis of Rayleigh-Bénard convection at large Rayleigh number. J. Fluid Mech. **178**, 53-71.

Jimenez, J. 2000 Turbulence. In: Perspectives in fluid dynamics, eds. G. K. Batchelor, H. K. Moffatt and M. G. Worster, pp. 231-288. C. U. P., Cambridge.

Krevor, S., Blunt, M.J., Benson, S.M., Pentland, C.H., Reynolds, C., Al-Menhali, A. and Niu, B., 2015. Capillary trapping for geologic carbon dioxide storage–From pore scale physics to field scale implications. International Journal of Greenhouse Gas Control, 40, pp.221-237.

Kolmogorov, A.N., 1941. The local structure of turbulence in incompressible viscous fluid for very large Reynolds numbers. Cr Acad. Sci. URSS, 30, pp.301-305.

Lasheras, J.C. and Choi, H., 1988. Three-dimensional instability of a plane free shear layer: an experimental study of the formation and evolution of streamwise vortices. J, Fluid Mech., 189, pp.53-86.

Linden, P. F. 2000 Convection in the environment. In: Perspectives in fluid dynamics, eds. G. K. Batchelor, H. K. Moffatt and M. G. Worster, pp. 289-345. C. U. P., Cambridge.

McBirney, A. R. and R. M. Noyes 1979 Crystallisation and layering of the Skaergaard intrusion. J. Petrol. **20**, 487-554.

Mondal, R., Benham, G., Christodoulides, P., Neokleous, N. and Kaouri, K. 2019 Modelling and optimisation of water management in sloping coastal aquifers with seepage, extraction and recharge. J. Hydrol. **571**, 471-484.

Morton, B. R., G. Taylor and J. S. Turner 1956 Turbulent gravitational convection from maintained and instantaneous sources. Proc. R. Soc. Lond. A**234**, 1-23.

Pope, S. B. 2000 Turbulent flows. Cambridge University Press.

Prandtl, L. 1925 Bericht uber untersuchungen zur ausgebildeten turbulenz. Zs. angew. Math. Mech., 5:136–139.

Reynolds, O. 1883 An experimental investigation of the circumstances which determine whether the motion of water shall be direct or sinuous, and of the law of resistance in parallel channels. Proc. R. Soc. Lond., 35(224-226), pp.84-99.

Roberts, G. O. 1979 Fast viscous Bénard convection. Geophys. Astrophys. Fluid Dynamics **12**, 235-272.

Schlichting, H., Gersten, K., Krause, E., Oertel, H. and Mayes, K. Boundary-layer theory, volume 7. Springer, 1960.

Turcotte, D. L. and E. R. Oxburgh 1967 Finite amplitude convection cells and continental drift. J. Fluid Mech. **28**, 29-42.

Turcotte, D. L. and G. Schubert 1982 Geodynamics: applications of continuum physics to geological problems. John Wiley, New York.

Turner, J. S. 1974 Double-diffusive phenomena. Ann. Rev. Fluid Mech. **6**, 37-54.

Turner, J. S. 1979 Buoyancy effects in fluids. C. U. P., Cambridge.

Vitagliano, V. and P. A. Lyons 1956 Diffusion coefficients for aqueous solutions of sodium chloride and barium chloride. J. Amer. Chem. Soc. **78** (8), 1,549-1,552.

Wager, L. R. and G. M. Brown 1968 Layered igneous rocks. Oliver and Boyd, Edinburgh.

Wegener, A. L. 1924 The origin of continents and oceans. 3rd ed., trans. J. G. A. Skerl. Methuen, London.

Ziegler, G. R., A. L. Benado and S. S. H. Rizvi 1987 Determination of mass diffusivity of simple sugars in water by the rotating disk method. J. Food. Sci. **52** (2), 501-502.

Woods, A.W., 2015. Flow in porous rocks. Cambridge University Press.